Energy and Buildings 91 (2015) 187–198

Contents lists available at ScienceDirect

Energy and Buildings

journal homepage: www.elsevier.com/locate/enbuild

A data-driven state-space model of indoor thermal sensation using occupant feedback for low-energy buildings

Xiao Chen [a], Qian Wang [a,*], Jelena Srebric [b]

[a] Department of Mechanical and Nuclear Engineering, The Pennsylvania State University, University Park, PA 16802, USA
[b] Department of Mechanical Engineering, University of Maryland, College Park, MD 20742, USA

ARTICLE INFO

Article history:
Received 17 October 2014
Received in revised form 11 January 2015
Accepted 20 January 2015
Available online 28 January 2015

Keywords:
Dynamic thermal sensation
Thermal comfort
Actual mean vote
State-space Wiener model
Occupant feedback
HVAC control for low-energy buildings

ABSTRACT

A data-driven state-space Wiener model was developed to characterize the dynamic relation between ambient temperature changes and the resulting occupant thermal sensation. In the proposed state-space model, the mean thermal sensation state variable is governed by a linear dynamic equation driven by changes of ambient temperature and process noise. The output variable, corresponding to occupant actual mean vote, is modeled to be a static nonlinearity of the thermal sensation state corrupted by sensor noise. A chamber experiment was conducted and the collected thermal data and occupants' thermal sensation votes were used to estimate model coefficients. Then the performance of the proposed Wiener model was evaluated and compared to existing thermal sensation models. In addition, an Extended Kalman Filter (EKF) was applied to use the real-time feedback from occupants to estimate a Wiener model with a time-varying offset parameter, which can be used to adapt the model prediction to environmental and/or occupant variability. Future studies can use this model to dynamically control the Heating Ventilating and Air Conditioning (HVAC) systems to achieve a desired level of thermal comfort for low-energy buildings with actual occupant feedback.

1. Introduction

Buildings account for 40% of U.S. energy consumption, and therefore many recent research studies emphasize energy efficiency, advanced control technologies, and occupant feedback. In particular, it is important to design a control system that minimizes energy consumption, while providing satisfactory thermal comfort for occupants. Existing control algorithms were often designed such that neutral temperatures were achieved based on Fanger's thermal comfort model [1,2]. However, such neutral-temperature based thermal control might not be adequate, by noting the possible discrepancy between Fanger's Predicted Mean Vote (PMV) and the occupant Actual Mean Vote (AMV) [3–7], as well as possible bias in the relationship between Fanger's PMV and predicted percentage of people dissatisfied (PPD) [8–10]. Furthermore, thermal perceptions of occupants could be affected by occupant behavior adjustment, physiological acclimatization and psychological habituation and expectation based on the adaptive thermal comfort theory [11–14].

Fanger's PMV and the adaptive thermal comfort model predict thermal sensation in a steady-state or quasi steady-state condition. However, occupants in actual buildings often encounter non-uniform or transient changes of ambient temperatures or air velocities. Such spatial or temporal non-uniformity could occur when occupants walk through building zones with different set-point temperatures or it could occur when occupants stay in a room with set-point temperatures changing with time, such as scheduled decrease or increase of temperature in commercial buildings. In recent years, there has been increasing interest in studying dynamic thermal sensation (DTS) models during transient conditions [15–25]. The response of human body to transient temperature changes via warm or cold cutaneous thermo-receptors was examined by Ring and de Dear [15], and de Dear et al. [16], where a model of thermo-receptor impulse frequency was proposed as a function of skin temperature and its derivative. By regression analysis of data obtained from experiments in the literature and from simulation of a physiological model of human thermoregulation, Fiala et al. developed a model for dynamic thermal sensation as a function of mean skin temperature and its rate of change [17,18]. Kaynakli and Kilic investigated the thermal interaction between human body and environment where the effect of clothing and air velocity was considered under transient conditions [19]. Zhang et al. studied local thermal sensation and local comfort of individual body parts under non-uniform and transient environments, as well as their impact on the whole

* Corresponding author. Tel.: +1 814 8658281; fax: +1 814 8659693.
E-mail address: quw6@psu.edu (Q. Wang).

http://dx.doi.org/10.1016/j.enbuild.2015.01.038
0378-7788/

body sensation and comfort [10–22]. Furthermore, Zolfaghari and Maerefat developed a new thermoregulatory bio-heat model to estimate skin temperature subject to transient environments [23]. Guan et al. investigated the thermal sensation changes in an automobile when temperature rises up and drops down very fast [24]. Hoppe proposed to use non-steady state models to characterize thermal comfort from indoor to cold outdoor conditions [25]. Additional work on thermal comfort in transient conditions can be found in the review papers [26,27]. Capabilities and limitations of the existing thermal comfort models were also reviewed in the literature [28]. The main limitation of these models results from the uncertainties in characterizing model input parameters and the transformation of physiological inputs into a comfort perception [28]. Developing a data-driven model, especially using real-time occupant feedback for model adaptation, could offer new opportunities to reduce these sources of model uncertainties and to more directly link the physiological inputs to the comfort perception.

This study developed a data-driven dynamic state-space Wiener model for occupant thermal sensation subjected to ambient temperature changes[1]. Compared to the existing literature on dynamic thermal sensation, the main advantage of the proposed state-space model lies in two aspects. First, rather than estimating parameters in describing the trajectory of thermal sensation with respect to time as conducted by Fiala et al. [17], this study estimated parameters of the dynamic model itself that governs the occupant thermal sensation. Thus, the proposed state-space model for thermal sensation is more suitable for the design of model-based thermal control to achieve a desired level of thermal sensation that could also be a moving target. Second, when the indoor environmental or occupant associated conditions deviate from the nominal condition conducted in the chamber experiment that was used to determine the nominal parameters of the proposed Wiener model, this study showed that a Wiener model with a time-varying offset parameter can be estimated through an EKF [30] to capture the variation of occupant thermal sensation. Such adaptivity of the proposed model is particularly useful when the model is applied to an indoor environment and occupant population that do not match the chamber experiment exactly. Since the proposed thermal sensation model is data or occupant feedback driven, it is referred to as an occupant-feedback based model.

2. Model

2.1. Assumptions

This study considered the air temperature change as the only control input to the proposed thermal sensation model, and also used it as the sole control variable in the chamber experiment. The only heat source in the chamber came from the heating or cooling supply and thus that the mean radiant temperature (MRT) followed the air temperature closely. The available humidifier was not used in the chamber experiment to simulate the indoor environmental conditions typical for buildings without humidification. The study did not explicitly evaluate how the change of humidity, air velocity, and occupant activity and clothing levels affect occupant thermal sensation as it would explode the number of experimental conditions. But instead, the study assumed that the aggregate effect of aforementioned significant factors on occupant thermal sensation was captured by an offset parameter in the proposed state-space Wiener model with a logistic output function. Other thermal or non-thermal factors were considered as process and sensor noise in the proposed state-space model.

Note that even though the MRT changed during the conducted step-up and step-down experiments by 9K and 7K respectively (see Fig. 2), these changes were gradual and applicable to all chamber surfaces. Therefore, it should be noted that the model is not applicable to chambers and indoor spaces with highly asymmetric radiant surfaces, recognized to influence the thermal sensation of human subjects. Nevertheless, the model and data-collection methodology can be extended to indoor spaces with highly asymmetric radiant surfaces that typically use hydronic systems, such as chilled ceilings and radiant heating elements. This extension would require additional experiments for data collection to calibrate the proposed state-space model for thermal sensation.

2.2. State-space model for thermal sensation

The dynamic thermal sensation driven by ambient temperature changes is essentially nonlinear. Thermal sensation could approximately be considered as linear around the neutral region. However, it gets saturated when it reaches hot or cold conditions. Consequently, this study considered a dynamic state-space model of a Hammerstein-Wiener structure, specifically a Wiener model for thermal sensation. The advantage of adopting a Wiener model is that the thermal sensation dynamic responses can be decomposed into a linear state equation and a nonlinear output equation. Logistic functions, which have an "S' shape, are particularly suitable for modeling the nonlinear output function for thermal sensation.

Consider a discrete time dynamic model defined as follows,

$$x(k+1) = \sum_{i=1}^{n} f_i \times x(k+1-i) + \sum_{j=1}^{m} g_j \times u(k+1-j-p) + e(k) \quad (1)$$

where k denotes the discrete-valued time index for which the sampling time should be chosen long enough to allow detection of physiological response, $x(k)$ denotes the mean thermal sensation state at time index k, $u(k)$ denotes the ambient temperature, p denotes input delay, and $e(k)$ denotes the process noise entering the state equation. It should be noted that the thermal sensation state defined in the empirical model (1) should correlate, but not necessarily coincide with the physiological thermal state of a human body. The parameter n and m determine the order of the auto-regression and dynamic regression, respectively, and the parameters f_i and g_j denote the corresponding auto-regression and dynamic linear regression coefficients. For any nonzero order n and m, the thermal sensation $x(k)$ is assumed to depend on the previous history.

The measurement of the mean thermal sensation by occupants, the subject actual mean vote $y(k)$, is then modeled as

$$y(k) = \frac{a}{\exp[-c - b \times (x(k) - r)] + 1} + d + v(k) \quad (2)$$

by considering a logistic output function, where $v(k)$ denotes the sensor/measurement noise. The parameters r, a, b, c, and d represent the regressor mean, output coefficient, dilation, translation, and output offset of a logistic function, respectively; altogether, they determine the shape of the nonlinear output curve.

In the remainder of the paper, the model including state equation (1) and output equation (2) is called the *Wiener-logistic Model*. To identify the model in (1) and (2), all parameters were first assumed to be constant and estimated via a nonlinear least-squares method (Gauss-Newton algorithm) using chamber experimental data. When the indoor environmental or occupant associated conditions deviate from the nominal condition conducted in the chamber experiment, this study considered a time-varying offset parameter in the Wiener-logistic model and applied an EKF [28]

[1] The material in this study was partially presented at the 2014 American Control Conference, June 4–6, 2014, Portland, OR, USA [29].

to estimate the thermal sensation state and the unknown time-varying offset parameter simultaneously using occupant feedback. The estimation was achieved by treating the time-varying offset parameter as an additional state variable.

3. Chamber experiment

3.1. Experiment facility

The chamber experiment with human subjects was approved by the Institutional Review Board at the Pennsylvania State University (IRB # 41077). The experiment was conducted in a climate chamber with its dimension shown in Fig. 1. This state-of-the-art simulation and testing facility is divided into two identical rooms and each room has its own HVAC unit. A HOBO U12 data logger was positioned in the middle of each room to measure air temperature and relative humidity. The temperature measurement error for the data logger is less than ± 0.35 °C from 0 °C to 50 °C, and the measurement error for the relative humidity is less than ± 2.5% from 10% to 90%.

A BlackGlobe Temperature Sensor for Heat Stress (BlackGlobe) was mounted at the same position as the HOBO U12 data logger. The BlackGlobe thermometer measures the globe temperature and determines the MRT using the globe temperature and local velocity. The globe temperature sensor has a time delay of approximately 20 to 30 min, resulting in slightly delayed accounting of changes in MRT, mostly relevant to the data collection after the step changes in the environmental temperatures. The thermistor interchangeability error of the BlackGlobe is less than ± 0.2 °C from 0 °C to 70 °C. Several anemometers were also scattered around to monitor air flow velocities at different locations in each room. In this experiment, all environmental parameters were controlled to be the same for both rooms of the climate chamber, and both rooms were used at the same time so that there was enough space to accommodate all the participants. Therefore, the chamber can be viewed as a single virtual room and subject votes from the two rooms were not differentiated.

3.2. Experiment design

The experiment was conducted in February, with outdoor temperature around 5 °C to 7 °C, and outdoor humidity level around 50%. There were two sessions in the experiment and each session lasted 2.5 h. The time history of the set-point temperature of the climate chamber used in the experiment is shown in Fig. 2. The chamber air temperature was controlled by the chamber HVAC system to follow the set point, and consequently was the MRT. In the first session, the room temperature set-point was initially set at 21 °C for 50 min, then raised to 30 °C for another 50 min, and reduced back to 21 °C again for the rest of the time of the session. Contrary to this "low-high-low" set-point pattern, a "high-low-high" pattern was used for temperature set points in the second session of the experiment, with the low temperature set at 23 °C. A different low temperature was chosen in the 2nd session instead of the original 21 °C in the 1st session since the large internal load made it impossible for the chamber temperature to drop from 30 °C to 21 °C within 50 min, even with the chamber cooling power set to its maximum.

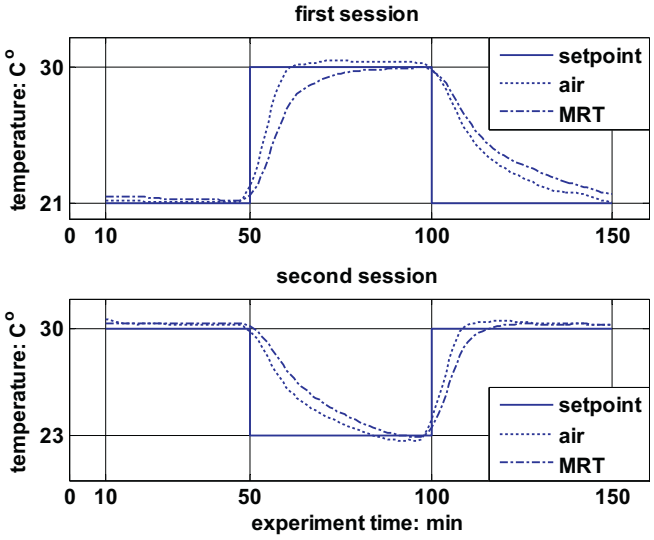

Fig. 2. Measured and set point air temperatures and mean radiant temperatures (MRT) during the experiment.

The experiment participants were requested not to take any spicy food or caffeinated drinks immediately before the start of the experiment. During the experiment, participants were allowed to work on laptops, read, and write in their sitting positions. Nobody walked in the chamber and nobody left the chamber during the

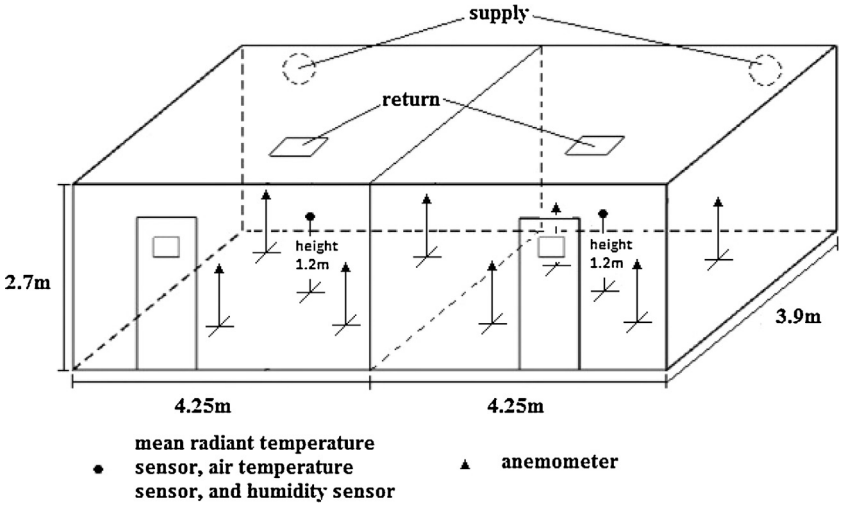

Fig. 1. Climate chamber layout. The chamber is divided into two identical rooms and each room has its own HVAC unit. A HOBO U12 is mounted in the middle of each room to measure air temperature and relative humidity, and a BlackGlobe sensor is mounted at the same position for MRT. Four anemometers are installed in each room to monitor air flow velocities. Both rooms are furnished with table and chairs for occupants to use.

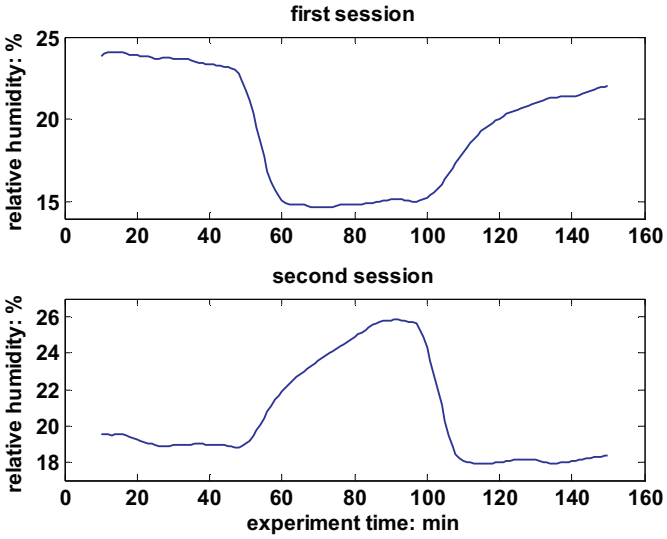

Fig. 3. Measured relative humidity (RH) during the experiment.

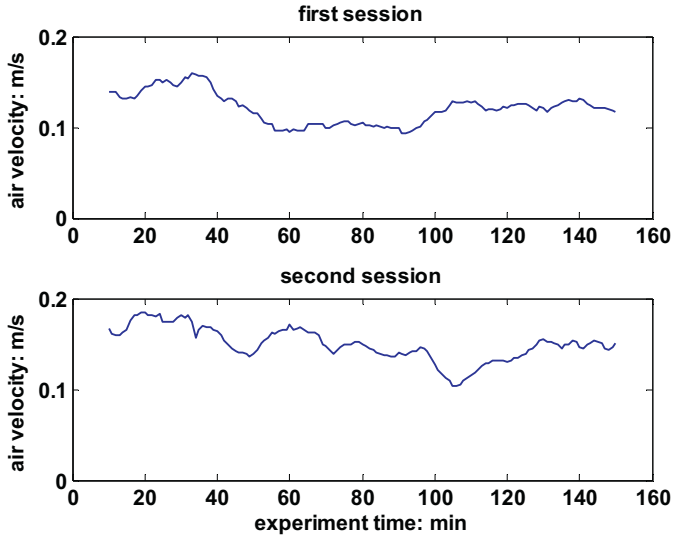

Fig. 4. Measured air velocities during the experiment.

experiment. An iButton sensor was attached to each participant to measure the skin temperature at hand. All participants were asked to write down their thermal sensation votes according to the ASHRAE 7-point thermal sensation scales every 5 min during a 20 min time period immediately after the initial change of air temperature set-point, and then every 10 min for the rest of the session time. Overall, more frequent sampling (every 5mins) was used to record the immediate sensation of participants after the chamber temperature was changed.

3.3. Data collection

There were a total of 13 participants, including college and graduate students[2], who completed both sessions of the chamber experiment. The recruitment of participants was not conducted to achieve a specific gender ratio and the recruited participants happened to consist of 12 male and 1 female. This relatively small number of participants is acceptable for this proof-of-concept development phase, which is a strategy used by other thermal comfort studies [7]. Further refinement and generalization of the proposed model require an extension of the present study to include data collection effort for a larger and more diverse population of occupants. Table 1 lists detailed information of each participant. The weight, height, age and gender of each participant were recorded to estimate each individual's basal metabolic rate. Clothing level of each subject was also recorded with detailed description. The activity level of each participant was considered sedentary since each participant was either reading or writing in a sitting position. All environmental parameters were collected and stored in data loggers during the experiment. The measured chamber air and mean radiant temperature, relative humidity, and air velocity are shown in Figs. 2–4, respectively. Since the two rooms have almost identical thermal parameters, average numbers between two rooms are used in Figs. 2–4.

Fig. 2 shows that the actual chamber temperature was more responsive to the step increase of the set point temperature than the step decrease of the set point temperature due to the capacity of the chamber HVAC system. Furthermore, the MRT followed the air temperature very closely as expected, where the visible delay

[2] College and graduate students were recruited since the NSF EFRI project, which sponsored the chamber experiment, aimed to evaluate building solutions for university campuses, where the recruited subjects are a representative population.

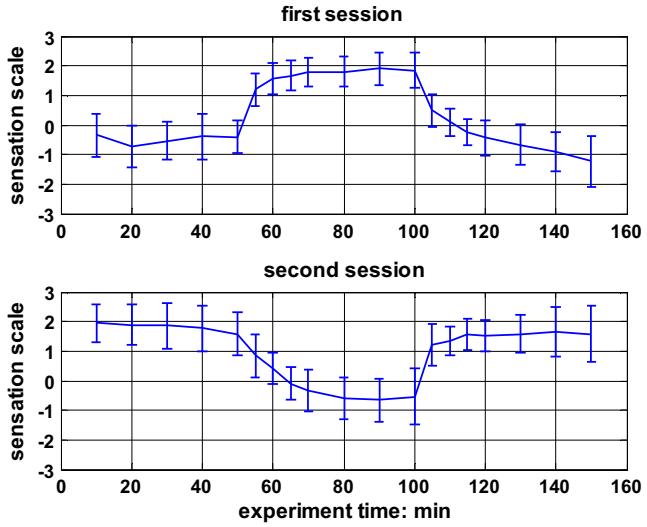

Fig. 5. Time series of occupant actual mean vote for thermal sensation along with standard deviation error bar.

of MRT is due to the time delay of the BlackGlobe temperature sensor. The humidity on the other hand showed a roughly flipped pattern of air temperature (shown in Fig. 3) because no additional humidification was supplied.

Fig. 5 shows the time series of subject actual mean vote for thermal sensation along with standard deviation error bar, where the ASHRAE 7-point scales [31] were used and Fig. 6 plots the corresponding subject votes on thermal comfort. The thermal comfort results include mean values together with standard deviation on a scale of −1 to 1, where −1, 0, and 1 correspond to very uncomfortable, just (un)comfortable, and very comfortable, respectively. The standard deviation of subject votes on thermal comfort is relatively large, which indicates the inhomogeneity of the subject group on thermal comfort perception.

4. Modeling results and analysis

4.1. Thermal sensation model with constant parameters

Among the two sessions for the chamber experiment, data from one session were used as training data to estimate model

Table 1
Participant's information.

ID	Weight (kg)	Height (m)	Age	Gender	Clothing
1	70.3	1.7	23	M	Pants, long-sleeve shirt, boots
2	104.3	1.93	23	M	Pants, long-sleeve shirt, shoes
3	86.2	1.93	19	M	Pants, short-sleeve shirt, shoes
4	97.5	1.85	22	M	Pants, short-sleeve shirt, sweatshirt, shoes
5	89.36	1.75	34	M	Pants, long-sleeve shirt, shoes
6	77.1	1.78	24	M	Pants, long-sleeve shirt, shoes
7	72.6	1.80	25	M	Athletic sweat pants, short-sleeve shirt, sweatshirt, shoes
8	71.7	1.85	26	M	Pants, long-sleeve shirt, shoes
9	72.1	1.70	27	M	Pants, long-sleeve shirt, shoes
10	64.7	1.75	22	M	Pants, short-sleeve and long-sleeve shirt, shoes
11	78	1.83	22	M	Pants, long-sleeve shirt, shoes
12	59.9	1.75	26	M	Athletic sweat pants, sweatshirt shoes
13	46.3	1.55	28	F	Pants, short-sleeve shirt, sweatshirt, shoes

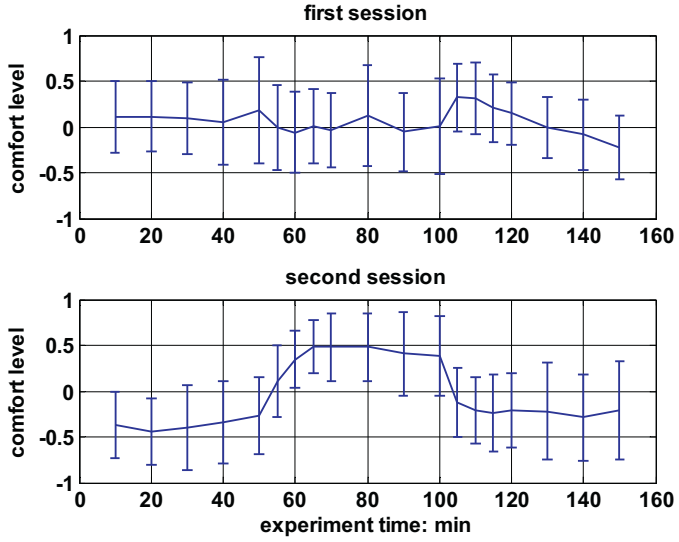

Fig. 6. Time series of occupant votes for thermal comfort along with standard deviation error bar.

parameters and data from the other session were used as validation data to evaluate the model predictions. Below we show the modeling results obtained by using the second session for training and the first session for model evaluation. Results from using the first session for training and second session for evaluation are omitted here due to the limited space. Since the collected measurements from occupants were not uniformly sampled, linear interpolation was used to generate additional votes. A nonlinear least-squares (Gauss-Newton) algorithm from MATLAB was applied to the training data, and the resulting discrete-time Wiener-logistic model (with a 5-min sampling time) is given as follows,

$$x(k+1) = 0.798 \times x(k) + 0.0610 \times x(k-1) + u(k) - 0.883 \times u(k-1) + e(k) \quad (3)$$

$$y(k) = \frac{3.033}{\exp\left[8.166 - 0.558 \times (x(k) - 7.931)\right] + 1} - 0.994 + v(k) \quad (4)$$

Two metrics, *mean-squared error* and *coefficient of determination* (R^2), were computed and given in Table 2, to quantify the goodness of fit for model prediction. Various model orders were tried for the linear state equation (3) and further increasing its order showed marginal improvement in goodness of fit. Figs. 7 and 8 illustrate the comparison of the model prediction by the Wiener-logistic model to the subject mean vote (denoted by "measured") from the second experiment session as training data (shown in Fig. 7) and from the first session as testing data (shown in Fig. 8). These results show

Table 2
Goodness of model fit and prediction in terms of mean-squared error (MSE) and coefficient of determination (R^2).

Model	Data	MSE	R^2
Wiener-Logistic	1st Session (testing)	0.0549	0.9537
	2nd Session (training)	0.0123	0.9856
Fanger's PMV	1st Session	0.6758	0.4294
	2nd Session	0.2066	0.7575
Modified Fiala's DTS	1st Session (entire session)	0.2403	0.8085
	Cooling segment of 1st Session	0.071	0.9321
	2nd Session (entire session)	0.4199	0.4807
	Warming segment of 2nd Session	0.2354	0.6940

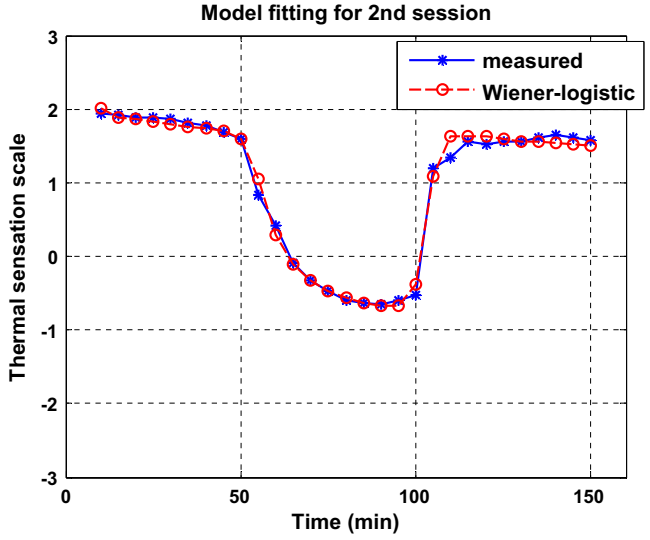

Fig. 7. Model estimation for thermal sensation using subject mean vote from the second session as training data.

that the Wiener-logistic model prediction follows the change of subject mean vote reasonably well.

4.2. Comparison to existing models

This study compared the prediction performance of the Wiener-logistic model to (1) Fanger's PMV model, and (2) a modified Fiala's model for dynamic thermal sensation. Though the PMV is a static model used for prediction of thermal sensation in a steady-state environment, this study still included the comparison for possible interest of readers since PMV is often used as comfort index in indoor thermal control design [1]. Fig. 9 shows comparison of the three models versus the time series of subject mean vote. Statistics

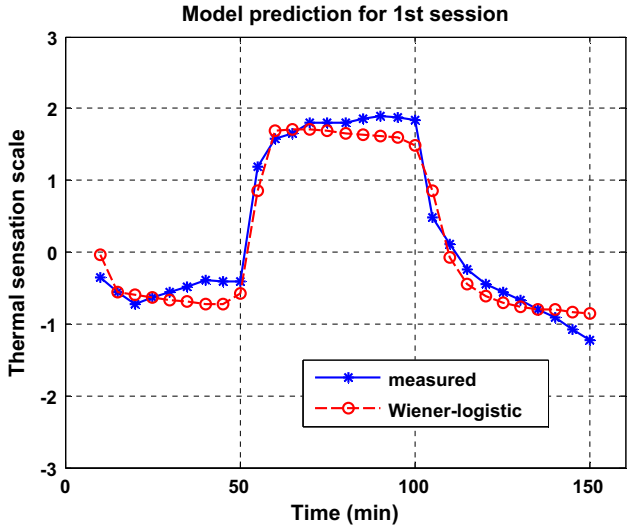

Fig. 8. Model validation for thermal sensation using subject mean vote from the first session as testing data.

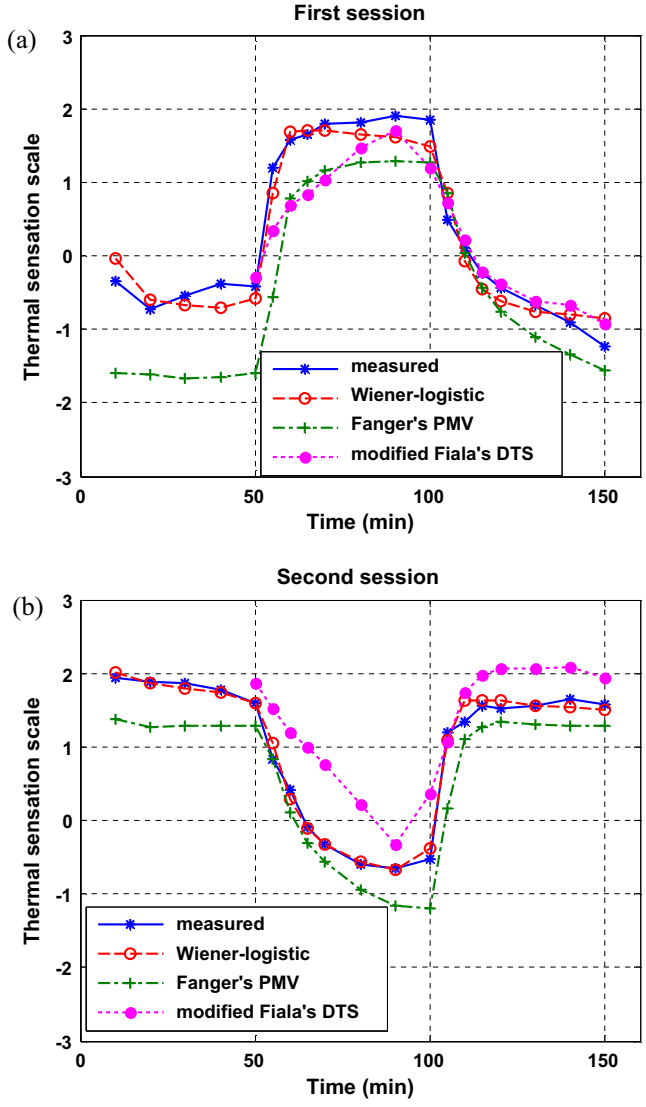

Fig. 9. Comparisons of the Wiener-logistic, Fanger's PMV, and a modified Fiala's DTS: (a) using time series of actual mean vote from the first session; (b) using time series of actual mean vote from the second session.

on the goodness of fit for the Fanger's PMV model and the modified Fiala's DTS model are given in Table 2 as well.

4.2.1. Fanger's PMV model

Fanger's PMV model used chamber environmental parameters and participants' clothing information (with a mean value of 0.71 being estimated using data from Table 1) to compute the prediction for thermal sensation. On one hand, Fig. 9 shows that during transient cooling periods, the Fanger's PMV tends to have a steeper slope than the actual subject mean vote and the Wiener-logistic model prediction. On the other hand, during transient warming, the PMV tends to have a relatively flatter slope than the actual subject mean vote and the Wiener-logistic model prediction as shown in Fig. 9(b). Though the PMV is very close to measurement results at several data points, overall the PMV underestimates the occupant thermal sensation. The subject mean vote has about 1 scale warmer sensation than the Fanger's PMV at the beginning of the first session, and a discrepancy of 0.6–0.9 scale that lasts until the thermal sensation reaches steady state. It is worth pointing out that for a mean monthly outdoor temperature of $T_m = 6\,^{\circ}\mathrm{C}$, the corresponding neutral temperature computed using the empirical formula by Humphreys [32] for climate-controlled buildings is $T_n = 23.9 + 0.295(T_m - 22)\exp(-((T_m - 22)/(24\sqrt{2}))^2) = 20.12^0C$, which agrees with the subject actual mean vote and the Wiener-logistic model prediction at the beginning of the first session where air temperature was set at 21 °C.

4.2.2. A modified Fiala's model

For sedentary subjects, the Fiala's model [17], given in Appendix A, predicts the dynamic thermal sensation in terms of the mean skin temperature and its rate of change. Since only the hand skin temperature, rather than the whole-body skin temperature, was measured in our experiment, this study replaced the mean skin temperature and its derivative in the Fiala's model by the hand skin temperature and derivative, and re-estimated the model regression coefficients using experimental data. The resulting model is a *modified Fiala's model*, given as follows:

$$DTS = 3 \times \tanh\left[0.1851 \times \Delta T_{\mathrm{hand}}^{(-)} + 0.2584 \times \Delta T_{\mathrm{hand}}^{(+)} + 3.850 \times 10^{-3} \times \frac{\mathrm{d}T_{\mathrm{hand}}^{(-)}}{\mathrm{d}t} + 1.780 \times 10^{-2} \times \exp\left(\frac{-0.4814 \times t}{3600}\right) \times \left(\frac{\mathrm{d}T_{\mathrm{hand}}^{(+)}}{\mathrm{d}t_{\max}}\right)\right] \quad (5)$$

where the first two terms in tanh(·) correspond to the static component, and the last two terms describe the dynamic component of the thermal sensation model. $\Delta T_{\mathrm{hand}}^{(+)}$ and $\Delta T_{\mathrm{hand}}^{(-)}$ denote the positive or negative deviation of local hand skin temperature from its reference value that gives the neutral thermal sensation; $\mathrm{d}T_{\mathrm{hand}}^{(-)}/\mathrm{d}t$ denotes the negative rate of change of hand skin temperature, and $\mathrm{d}T_{\mathrm{hand}}^{(+)}/\mathrm{d}t_{\max}$ denotes the maximum positive rate of change of hand skin temperature. The time t denotes the elapsed time since the occurrence of $\mathrm{d}T_{\mathrm{hand}}^{(+)}/\mathrm{d}t_{\max}$. In modeling the thermal sensation during warming, $\Delta T_{\mathrm{hand}}^{(-)}$ and $\mathrm{d}T_{\mathrm{hand}}^{(-)}/\mathrm{d}t$ are set to zero, and in modeling the thermal sensation during cooling, $\Delta T_{\mathrm{hand}}^{(+)}$ and $\mathrm{d}T_{\mathrm{hand}}^{(+)}/\mathrm{d}t_{\max}$ are set to zero.

Since it took a long warm up period for the sensor to be able to measure subject hand temperature accurately, subject hand temperature measurements were not available until $t = 50$ min after the

experiment started. Therefore, in order to have a sufficient number of data points to estimate the regression coefficients of the modified Fiala's model, this study used all data from both sessions as training data. Fig. 9 shows that the modified Fiala's model does not do well at the beginning (50 min < t < 90 min) of each session, which could be due to lack of a sufficient number of data points for parameter estimation. For 90 min < t < 150 min, predictions of the modified Fiala's model match the observed mean vote pretty well for cooling, but they have slightly less than 0.5 scale over estimation for warming. Furthermore, Fig. 9 shows that during the transient cooling (2nd segment of Fig. 9(a)), the curve slope of the modified Fiala's model is closer to the curve slope of the actual subject mean vote than that of the Wiener-logistic model and the PMV. However, during the transient warming (2nd segment of Fig. 9(b)), the curve slope of the modified Fiala's model is slightly flatter than that of the actual subject mean vote and the Wiener-logistic model.

The statistics in Table 2 demonstrate a similar trend revealed by Fig. 9. Besides the session-wise goodness of fit, separate metrics were calculated for the cooling segment of 1st session and the warming segment of 2nd session, respectively, noting that the session-wise fitness values could be relatively low due to an insufficient number of data points at the warming segment of 1st session and the cooling segment of 2nd session. Table 2 shows that for the cooling segment of 1st session, the modified Fiala's model has a very close R^2 value to that of the Wiener-logistic model for the 1st session. However, for the warming segment of 2nd session, the Wiener-logistic model has 40% higher R^2 than the modified Fiala's model.

4.3. Using occupant feedback to improve model predictions

4.3.1. Time-varying thermal sensation model

In the thermal sensation model (3–4), this study considered air temperature as the sole control input and explicitly modeled its effect on the occupant thermal sensation. The effects of other significant environmental input variables, such as the relative humidity and air velocity, and the effects of occupant clothing levels and metabolic rates were considered to be captured by an aggregate parameter—the offset parameter in the Wiener-logistic model. Therefore, the proposed model neither included these parameters individually nor explicitly.

This study also showed through simulations that by considering a time-varying offset parameter d in the Wiener-logistic model (2) and estimating it in real time via an EKF [30], it is possible to capture the variation of occupant thermal sensation due to: Case I) the change of relative humidity, and Case II) the change of occupant clothing level. Basically, the time-varying offset parameter $d(t)$ serves as a correction term for predictions of occupant thermal sensation when one or multiple un-modeled environmental or occupant-associated inputs deviate from their nominal values being used in training datasets for model calibration. In the implementation of the EKF, the unknown time-varying offset parameter was treated as a new state variable modeled by a random process driven by an additional process noise. Then this new state variable was added to the thermal sensation state to form an augmented state and the EKF was applied to estimate the augmented state. The details of using EKF for simultaneous estimation of the state variable and unknown model coefficient (i.e., the augmented state) are given in Appendix B. Furthermore, this study also showed that a continuously changing offset parameter is not necessary. The consistency check of the EKF can automatically detect the change of environmental and/or occupant disturbance input with a statistically significant magnitude and then a new offset parameter d can be estimated to effectively correct the model prediction of thermal sensation.

Since variations of relative humidity or occupant clothing level were not controlled in the chamber experiments, rather than using actual occupant votes, this study used the PMV with added zero mean Gaussian noise to simulate the occupant votes and referred to them as the *virtual occupant's feedback*. The added Gaussian noise was intended to reflect possible sensing noise between the PMV and occupant AMV. The Gaussian noise was considered to have zero mean by assuming that the PMV was not biased in predicting occupant thermal sensation. In both cases described below, the parameters (except the relative humidity and clothing level) used to run the PMV model are given as follows: air temp = 25.85 °C, MRT = 25.85 °C, air velocity = 0.135 m/s, and activity level = 1.

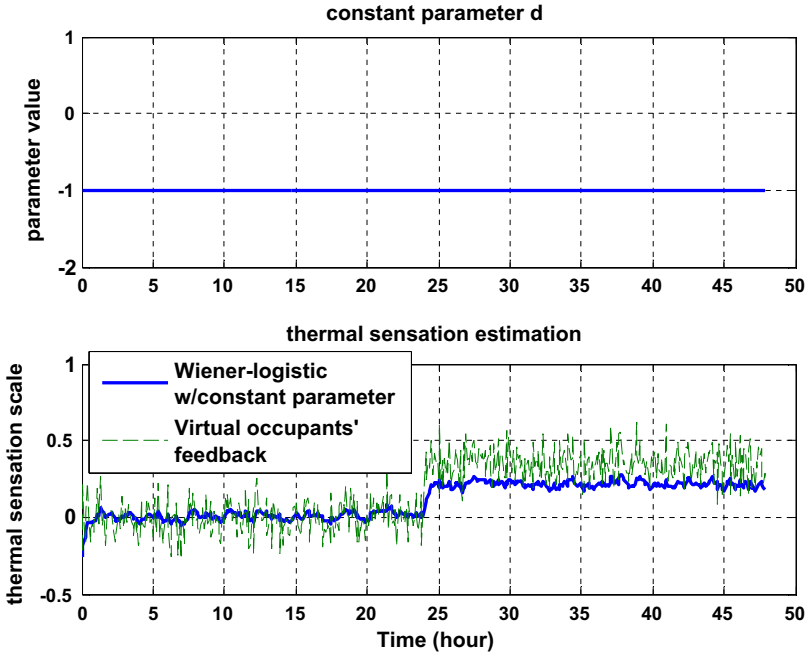

Fig. 10. Wiener-logistic model with constant offset parameter, where the relative humidity changes from 21% to 60% at t = 24 h.

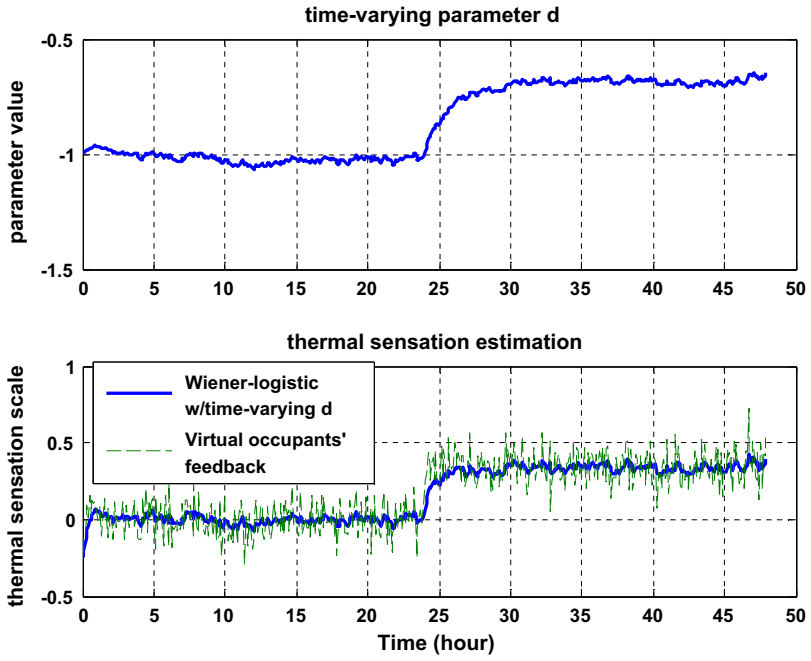

Fig. 11. Wiener-logistic model with time-varying offset parameter, where the RH changes from 21% to 60% at $t = 24$ h.

4.3.1.1. Case I: Change of relative humidity level. For this case, the occupant clothing level was maintained to be 0.71. The relative humidity (RH) was set to RH = 21% for the first 24 h, and changed to RH = 60% from $t = 24$ h to $t = 48$ h. The Gaussian noise variance in simulating the virtual occupant feedback was set to be 0.03. The process and measurement noise variances in implementing the Kalman filter were set to be 0.005 and 0.03, respectively. Fig. 10 shows that for a constant offset parameter $d = -1$, the predicted sensation by the Wiener-logistic model is close to the mean of virtual occupant votes at near neutral thermal sensation when RH = 21%. However, when RH increases to 60% at $t = 24$ h, the predicted sensation is around 0.2 scale lower than the mean of virtual occupant votes. In Fig. 11, a time-varying offset parameter d is considered for the Wiener-logistic model and the artificial noise variance for d is tuned such that the consistency of the EKF is achieved (detailed discussions are given in Section 4.3.2). These results show that d increases to around -0.75 in response to the RH increase, and the resulting model prediction is able to capture the thermal sensation variation due to the increase of RH.

4.3.1.2. Case II: Change of occupant clothing level. For this case, the relative humidity was maintained at RH = 21%. The clothing level was kept at 0.71 (this was the averaged value in the chamber experiments) for the first 24 h and then decreased to 0.4 from

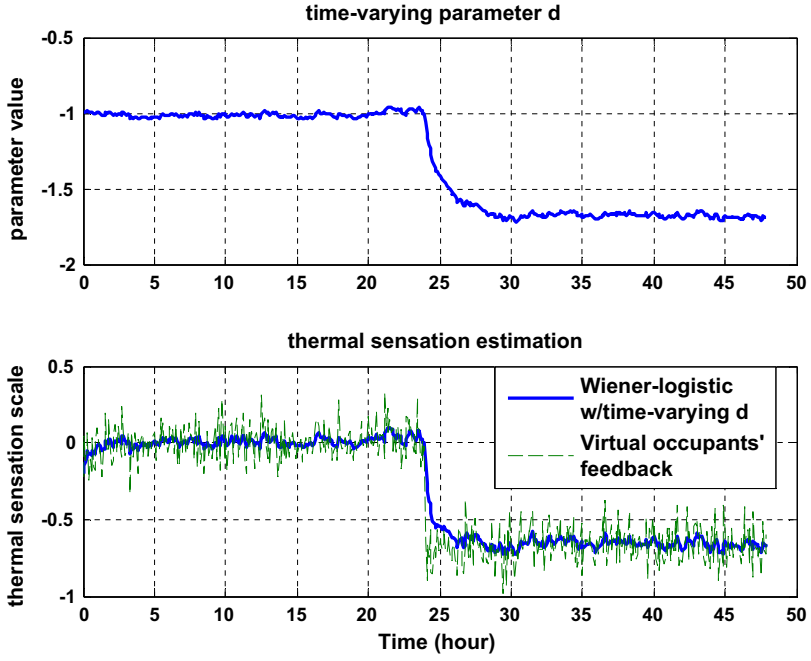

Fig. 12. Wiener-logistic model with time-varying offset parameter, where the clothing level changes from 0.71 to 0.4 at $t = 24$ h.

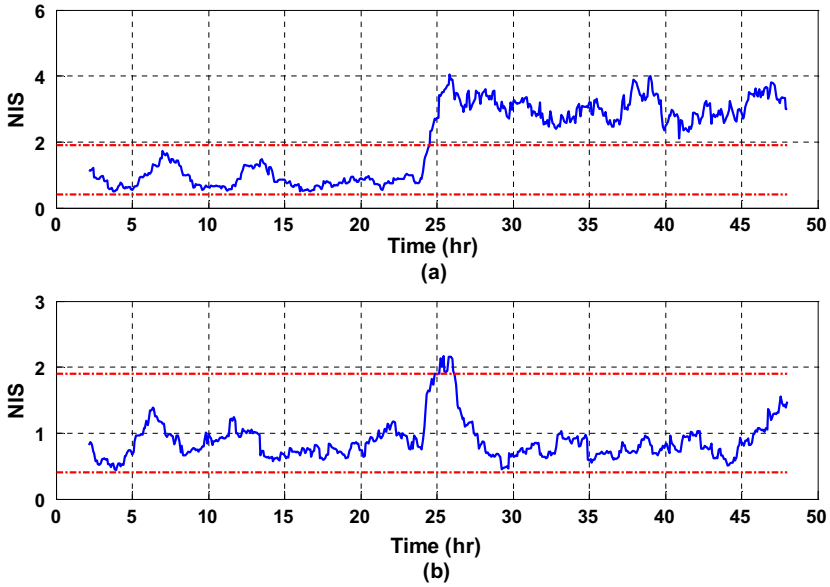

Fig. 13. Moving average normalized innovation squared (NIS) with its 99% probability region, where the relative humidity changes from 21% to 60% at $t = 24$ h. (a) Wiener-logistic model with constant d; (b) Wiener-logistic model with time-varying d.

$t = 24$ h to $t = 48$ h. The Gaussian noise variance in simulating the virtual occupant feedback was set to be 0.01. The process and measurement noise variances in implementing the Kalman filter were set to be 0.005 and 0.01, respectively. Fig. 12 illustrates that the Wiener-logistic model with time varying offset parameter is able to capture the effects on occupant thermal sensation due to a sudden change of occupant's clothing level at $t = 24$ h by reducing d from −1 to around −1.7.

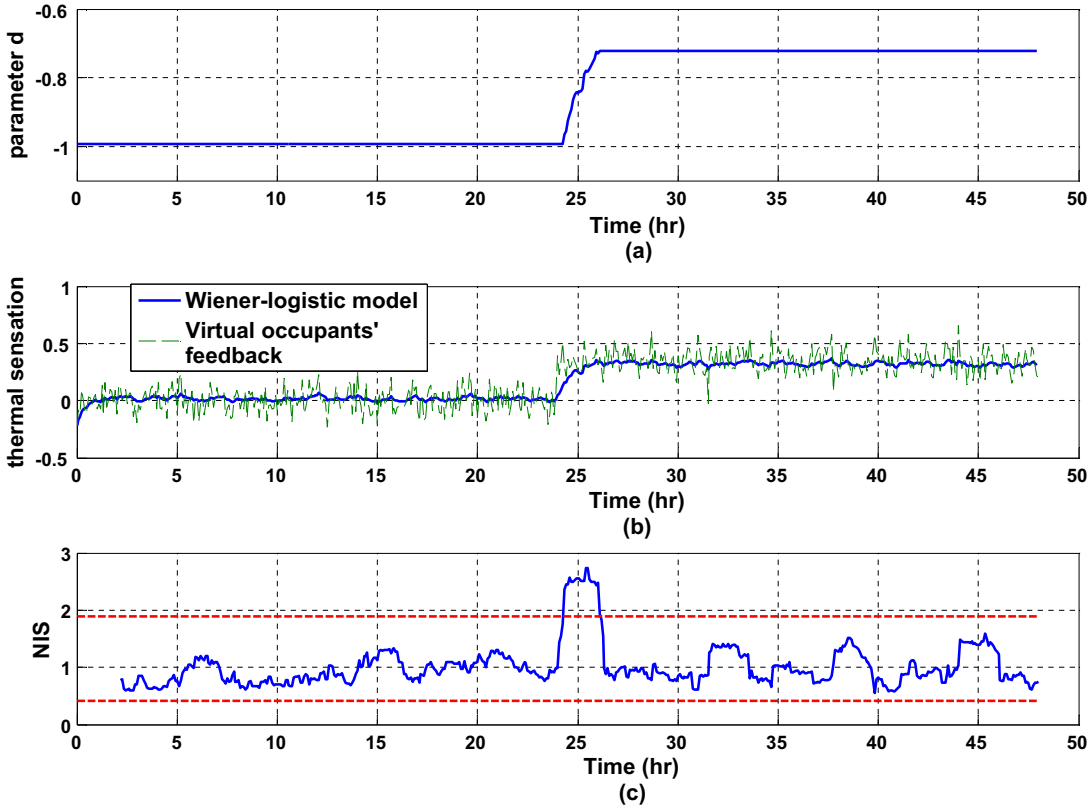

Fig. 14. Wiener-logistic model with piece-wise constant d, where the relative humidity changes from 21% to 60% at $t = 24$ h. (a) parameter d; (b) model predicted thermal sensation versus virtual occupant votes; (c) moving average normalized innovation squared (NIS).

4.3.2. Consistency of Kalman filter

Capturing the thermal sensation variation due to non-negligible changes in the un-modeled environmental or occupant disturbance inputs through estimating the time-varying offset parameter d by EKF requires monitoring the consistency of the Kalman filter. Essentially, when such changes occur, under the original nominal offset parameter d, the consistency of EKF will be violated, and re-estimation of a new offset parameter d is needed to regain the filter consistency.

The consistency of a Kalman filter can be verified by Chi-square test of whiteness of the innovation sequence. The Normalized Innovation Squared (NIS) is defined as:

$$\varepsilon_\nu(k) = \nu(k)'S(k)^{-1}\nu(k) \tag{6}$$

where the innovation ν is the difference of the measurement (corresponding to occupant feedback here) and the filter predicted measurement, and S denotes the filter calculated innovation covariance [20]. To reduce the variability, a moving average of NIS over a sliding window of size w can be used and it is defined as,

$$\varepsilon_\nu^w(k) = \frac{1}{w} \times \sum_{j=k-w+1}^{k} \varepsilon_\nu(j) \tag{7}$$

where $w \cdot \varepsilon_\nu^w(k)$ is assumed to be Chi-square distributed with $w \cdot n_z$ degree of freedom, n_z denotes the dimension of the measurement and it is equal to 1 for the thermal sensation model.

The analysis of filter consistency for *Case I* is presented here, while the filter consistency check for *Case II* can be conducted in a similar way and thus is omitted. Consider a window size of $w = 24$ in (7), which corresponds to collecting feedback from occupants every 5 min for two hours. This study first checked the filter consistency corresponding to the Wiener-logistic model with a fixed offset parameter $d = -1$. Evaluation of the two-sided 99% Chi-square distribution with a degree of freedom $n_z = 24$ indicates that the filter is consistent if $w \cdot \varepsilon_\nu^w(k) \in [9.886, 45.559]$ or $\varepsilon_\nu^w(k) \in [0.4119, 1.8983]$, which is referred to as the 99% probability (or acceptance) region. Fig. 13(a) shows that the filter is consistent for the first 24 h, but not for the second 24 h. This is confirmed by Fig. 10 that from $t = 24$ h to $t = 48$ h, the predicted sensation is around 0.2 scale lower than the mean of virtual occupant votes and thus the expected value of the innovation sequence is not zero any more. Next, consider the Wiener-logistic model with a time varying parameter d whose value was estimated by an EKF (shown in Fig. 11), Fig. 13(b) shows that the corresponding moving average NIS is within the 99% probability bounds till $t = 25.16$ h, when the filter consistency is lost, but the NIS comes back to the acceptance region after $t = 26.15$ h to regain the filter consistency.

A relatively simple alternative to the continuously changing offset parameter d is a piece-wise constant d, i.e., start with the Wiener-logistic model with a constant offset parameter and only re-estimate a new d when the NIS goes outside its acceptance region. Fig. 14 shows that the moving average NIS exceeds the upper bound of its 99% probability region [0.4119, 1.8983] at $t = 24$ h, which corresponds to the change of RH from 21% to 60%. Then the offset parameter d is re-estimated by EKF and a new value of $d = -0.7224$ is obtained at $t = 26.25$ h to regain the filter consistency. The difference between the model in Fig. 14 and the one in Fig. 13 is that once a new offset parameter d is obtained to regain the filter consistency, continuously updating its value via EKF is not needed until the filter consistency is lost again.

5. Conclusion

This study developed an empirical state-space model of the Hammerstein–Wiener structure, specifically a Wiener model with logistic output function, for thermal sensation resulting of ambient temperature changes. The model takes air temperature as input, and defines mean thermal sensation as a state variable, and the occupant actual mean vote as an output. A chamber experiment provided thermal data and occupant thermal sensation votes to estimate the model coefficients. Comparison of the developed Wiener-logistic model to the classic Fanger's Predicted Mean Vote (PMV) model and a modified Fiala's model for dynamic thermal sensation was conducted. The Wiener-logistic model has a comparable R^2 value to the modified Fiala's model for predicting thermal sensation during cooling, but has a significantly higher R^2 than the modified Fiala's model for predicting thermal sensation during warming. This indicates that the proposed Wiener-logistic model could be a promising alternative to the Fiala's model. By considering a Wiener-logistic model with a time-varying offset parameter estimated by an Extended Kalman Filter (EKF) using occupant feedback, this study also showed that when indoor environmental or occupant associated conditions deviate from the nominal condition conducted in the chamber experiment, the consistency check of the EKF can automatically detect the changes, and re-estimation of the offset parameter can effectively correct the model predictions of thermal sensation. We expect that the proposed empirical thermal sensation model can be used in the design of occupant-oriented indoor thermal control, as a replacement or a complementary modeling tool to the traditional PMV model.

This study had a relatively small number of human subjects in the conducted chamber experiment. In addition, the participants were primarily young male, corresponding to the same boundary condition as Fanger's comfort studies with young subjects. Thus when the model is applied to a different group and size of human subjects, it could possibly lead to numerical errors in the developed model parameters. However, by allowing the offset parameter of the proposed model to be time varying, the model can be updated for any new applications by an EKF using new additional data whenever they are available. Overall, the developed data-driven state-space model of thermal sensation provides ample opportunities for improvements with additional datasets as all data-driven models do. In addition, in this particular application, there is an opportunity to simultaneously save energy and improve thermal comfort in support of low-energy buildings.

Acknowledgements

This work is supported by National Science Foundation under-NSF grant EFRI-1038264/EFRI-1452045. We also would like to thank Dr. Moshood O. Fadeyi, Dr. Mohammad Heidarinejad and Dr. Mingjie Zhao for the help with the chamber experiments.

Appendix A. Fiala's dynamic thermal sensation model

Fiala's model for predicting dynamic thermal sensation for sedentary subjects, in terms of the 7-point ASHRAE scale from −3 to +3, is given as follows:

$$DTS = 3 \times \tanh\left[0.3 \times \Delta T_{sk,m}^{(-)} + 1.08 \times \Delta T_{sk,m}^{(+)} + 0.11 \times \frac{dT_{sk,m}^{(-)}}{dt} + 1.91 \times \exp\left(\frac{-0.681 \times t}{3600}\right) \times \frac{dT_{sk,m}^{(+)}}{dt_{\max}}\right] \tag{A.1}$$

where $\Delta T_{sk,m}^{(-)}$ and $\Delta T_{sk,m}^{(+)}$ denote the negative and positive deviation of the mean skin temperature from its reference temperature corresponding to neutral thermal sensation; $dT_{sk,m}^{(-)}/dt$ and $dT_{sk,m}^{(+)}/dt$ denote the negative and positive time derivative of the mean skin temperature, respectively. The dynamic component of this model for skin cooling, represented by $0.11 \times dT_{sk,m}^{(-)}/dt$, is modeled differently from skin warming, which is described by the maximum positive rate of change of skin temperature, $dT_{sk,m}^{(+)}/dt_{\max}$, multiplying an exponentially decaying coefficient $\exp(-0.681t/3600)$, where t denotes the time elapsed since the occurrence of $dT_{sk,m}^{(+)}/dt_{\max}$.

Appendix B. Extended Kalman Filter for estimating thermal sensation and time-varying model parameters simultaneously

Consider the Wiener-logistic thermal sensation model (3–4),

$$x(k+1) = f_1 x(k) + f_2 x(k-1) + g_1 u(k) + g_2 u(k-1) + e(k) \tag{B.1}$$

$$y(k) = \frac{a}{\exp\left[-c - b \times (x(k) - r)\right] + 1} + d + v(k) \tag{B.2}$$

where the model coefficients $f_1, f_2, g_1, g_2, a, b, c, r$ are constant and defined accordingly. We assume that the offset parameter d is slowly time-varying and modeled as a (discrete time) wiener process as follows:

$$d(k+1) = d(k) + e_d(k) \tag{B.3}$$

where the parameter process noise e_d is assumed to have zero mean and nonzero variance Q_d.

Define an augmented state variable $x_A(k)$ consisting of the original state variable $x(k)$, $x(k-1)$, and the time-varying parameter $d(k)$,

$$x_A = \begin{bmatrix} x_{A_1} \\ x_{A_2} \end{bmatrix}, \quad x_{A_1} = \begin{bmatrix} x_{A_1}^1 \\ x_{A_1}^2 \end{bmatrix} \triangleq \begin{bmatrix} x(k) \\ x(k-1) \end{bmatrix},$$
$$x_{A_2}(k) \triangleq d(k) \tag{B.4}$$

Then the original thermal sensation model (Eqs. (B.1) and. (B.2)) together with the parameter model (Eq. (B.3)) can be rewritten as follows,

$$\begin{aligned} x_A(k+1) &= F x_A(k) + G \circ u(k) + \varepsilon(k) \\ y(k) &= h(x_A(k)) + v(k) \end{aligned} \tag{B.5}$$

where $G \circ u(k) = \begin{bmatrix} g_1 u(k) + g_2 u(k-1) & 0 & 0 \end{bmatrix}^T$, $\varepsilon(k) = \begin{bmatrix} e(k) & 0 & e_d(k) \end{bmatrix}^T$, the matrix F satisfies

$$F = \begin{bmatrix} f_1 & f_2 & 0 \\ 1 & 0 & 0 \\ 0 & 0 & 1 \end{bmatrix} \tag{B.6}$$

and the output nonlinear function $h(x_A(k)) = a / \left(\exp(-c - b\left(x_{A_1}^1(k) - r\right)\right) + 1\right) + x_{A_2}(k)$.

The process noise $\varepsilon(k)$ and sensor noise $v(k)$ are assumed to be white noise and satisfy the following,

$$\begin{aligned} &E[\varepsilon(k)] = 0, E[\varepsilon(k)\varepsilon^T(k')] = Q(k)\delta_{kk'} \\ &E[v(k)] = 0, E[v(k)v^T(k')] = R(k)\delta_{kk'} \end{aligned} \tag{B.7}$$

It is assumed that the initial estimate $\hat{x}_A(0|0)$ is uncorrelated with the process noise and sensor noise sequences. Assume that one has the estimate at time k, $\hat{x}_A(k|k) = E[x_A(k)|Z^k]$ with the associate covariance matrix $P(k|k)$, where Z^k denotes the statistics obtained at time k.

The predicted state at time $k+1$ based on time k is obtained as follows,

$$\hat{x}_A(k+1|k) = F\hat{x}_A(k|k) + G \circ u(k) \tag{B.8}$$

The state prediction covariance is updated as

$$P(k+1|k) = FP(k|k)F^T + Q(k) \tag{B.9}$$

The predicted measurement for the 2nd-order Kalman filter is given by,

$$\hat{y}(k+1|k) = h(\hat{x}_A(k+1|k)) + \frac{1}{2} tr\left[h_{x_A x_A}(k+1)P(k+1|k)\right] \tag{B.10}$$

and the measurement prediction covariance matrix is updated as

$$\begin{aligned} S(k+1) &= h_{x_A}(k+1)P(k+1)h_{x_A}^T(k+1) \\ &+ \frac{1}{2} tr\left[h_{x_A x_A}(k+1)P(k+1|k)h_{x_A x_A}(k+1)P(k+1|k)\right] + R(k+1) \end{aligned} \tag{B.11}$$

where h_{x_A} and $h_{x_A x_A}$ denote the Jacobian and Hessian of the nonlinear function h, respectively,

$$\begin{aligned} h_{x_A}(k+1) &= [\nabla_{x_A} h(x_A)]^T|_{x_A = \hat{x}_A(k+1|k)}, h_{x_A x_A}(k+1) \\ &= [\nabla_{x_A} \nabla_{x_A}^T h(x_A)]|_{x_A = \hat{x}_A(k+1|k)} \end{aligned} \tag{B.12}$$

References

[1] R. Freire, G. Oliveira, N. Mendes, Predictive controllers for thermal comfort optimization and energy savings, Energy Build. 40 (2008) 1353–1365.
[2] F. Oldewurtel, A. Parisio, C. Jones, D. Gyalistras, M. Gwerder, V. Stauch, B. Lehmann, M. Morari, Use of model predictive control and weather forecasts for energy efficient building climate control, Energy Build. 45 (2012) 15–27.
[3] R. de Dear, L. Leow, S. Foo, Thermal comfort in the humid tropics: field experiments in air-conditioned and naturally ventilated buildings in Singapore, Int. J. Biometeorol. 34 (4) (1991) 259–265.
[4] J. Busch, A tale of two populations: thermal comfort in air-conditioned and naturally ventilated offices in Thailand, Energy Build. 18 (3) (1992) 235–249.
[5] G. Schiller, A comparison of measured and predicted comfort in office buildings, ASHRAE Trans. 96 (1) (1990) 609–622.
[6] N. Wong, S. Khoo, Thermal comfort in classrooms in the tropics, Energy Build. 35 (4) (2003) 337–351.
[7] G. Brager, R. De Dear, Thermal adaptation in the built environment: a literature review, Energy Build. 27 (1) (1998) 83–96.
[8] V. Araujo, E. Araujo, The applicability of ISO 7730 for the assessment of the thermal conditions of users of the buildings in Natal-Brazil, Indoor Air 2 (1999) 148–153.
[9] D.W. Yoon, J.Y. Sohn, K.H. Cho, The comparison on the thermal comfort sensation between the results of questionnaire survey and the calculation of the PMV values, Indoor Air 2 (1999) 131–141.
[10] J. Van Hoof, Forty years of Fanger's model of thermal comfort: comfort for all? Indoor Air 18 (3) (2008) 182–201.
[11] R. de Dear, G. Brager, Developing an adaptive model of thermal comfort and preference, ASHRAE Trans. 104 (1) (1998) 145–167.
[12] R. de Dear, G. Brager, Thermal comfort in naturally ventilated buildings: revisions to ASHRAE Standard 55, Energy Build. 34 (6) (2002) 549–561.
[13] P. Fanger, J. Toftum, Extension of the PMV model to non-air-conditioned buildings in warm climates, Energy Build. 34 (6) (2002) 533–536.
[14] J. Nicol, M. Humphreys, Adaptive thermal comfort and sustainable thermal standards for buildings, Energy Build. 34 (6) (2002) 563–572.
[15] J. Ring, R. de Dear, Temperature transients: a model for heat diffusion through the skin, thermoreceptor response and thermal sensation, Indoor Air 1 (4) (1991) 448–456.
[16] R. de Dear, J. Ring, P. Fanger, Thermal sensations resulting from sudden ambient temperature changes, Indoor Air 3 (3) (1993) 181–192.
[17] D. Fiala, K. Lomas, M. Stohrer, First principles modeling of thermal sensation responses in steady-state and transient conditions, ASHRAE Trans. 109 (1) (2003) 179–186.
[18] D. Fiala, K. Lomas, M. Stohrer, A computer model of human thermoregulation for a wide range of environmental conditions: the passive system, J. Appl. Physiol. 85 (5) (1999) 1957–1972.
[19] O. Kaynakli, M. Kilic, Investigation of indoor thermal comfort under transient conditions, Build. Environ. 40 (2) (2005) 165–174.

[20] C. Huizenga, H. Zhang, E. Arens, D. Wang, Skin and core temperature response to partial-and whole-body heating and cooling, J. Therm. Biol. 29 (7) (2004) 549–558.
[21] H. Zhang, E. Arens, C. Huizenga, Thermal sensation and comfort models for non-uniform and transient environments: Part I: Local sensation of individual body parts, Build. Environ. 45 (2) (2010) 380–388.
[22] H. Zhang, E. Arens, C. Huizenga, Thermal sensation and comfort models for non-uniform and transient environments: Part II: Local comfort of individual body parts, Build. Environ. 45 (2) (2010) 389–398.
[23] A. Zolfaghari, M. Maerefat, A new simplified thermoregulatory bioheat model for evaluating thermal response of the human body to transient environments, Build. Environ. 45 (10) (2010) 2068–2076.
[24] Y. Guan, B. Jones, T. Gielda, M. Hosni, Investigation of human thermal comfort under highly transient conditions for automotive applications: Part 2: Thermal sensation modeling, ASHRAE Trans. 109 (2) (2003) 898–907.
[25] P. Hoppe, Different aspects of assessing indoor and outdoor thermal comfort, Energy Build. 34 (6) (2002) 661–665.
[26] J. Hensen, Literature review on thermal comfort in transient conditions, Build. Environ. 25 (4) (1990) 309–316.
[27] Y. Chen, J. Niu, N. Gao, Thermal comfort models: a review and numerical investigation, Build. Environ. 47 (2012) 13–22.
[28] B. Jones, Capabilities and limitations of thermal models for use in thermal comfort standards, Energy Build. 34 (6) (2002) 653–659.
[29] X. Chen, Q. Wang, J. Srebric, M.O. Fadeyi, Data-driven state-space modeling of indoor thermal sensation using occupant feedback, in: Proceedings of American Control Conference, June 4–6, Portland, OR, 2014, pp. 1710–1715.
[30] Y. Bar-Shalom, X. Li, T. Kirubarajan, Estimation with Applications to Tracking and Navigation, John Wiley & Sons, New York, NY, 2001.
[31] ASHRAE, ASHRAE standard, standard 55-2013, in: Thermal Environmental Conditions for Human Occupancy, 2013.
[32] M.A. Humphreys, Outdoor temperatures and comfort indoors, Build. Res. Pract. 6 (2) (1978) 92.